IEEE Access
Multidisciplinary | Rapid Review | Open Access Journal

Received August 4, 2019, accepted August 18, 2019, date of publication August 28, 2019, date of current version September 18, 2019.

Digital Object Identifier 10.1109/ACCESS.2019.2937940

Research on Dynamic Load-Sharing Characteristics of Two-Stage Asymmetric Star Gear System

MO SHUAI[1,2,3], MA SHUAI[1,2], JIN GUO GUANG[1,2], AND YUE ZONG XIANG[1,2]

[1]School of Mechanical Engineering, Tianjin Polytechnic University, Tianjin 300387, China
[2]Tianjin Key Laboratory of Advanced Mechatronics Equipment Technology, Tianjin 300387, China
[3]State Key Laboratory of Materials Processing and Die and Mould Technology, Huazhong University of Science and Technology, Wuhan 430074, China

Corresponding author: Mo Shuai (moshuai2010@163.com)

This work was supported in part by the National Natural Science Foundation of China under Grant 51805368, in part by the Natural Science Foundation of Tianjin under Grant 17JCQNJC04300, in part by the Open Funding of the State Key Laboratory of Materials Processing and Die and Mould Technology, Huazhong University of Science and Technology, under Grant P2019-022, in part by the Young Elite Scientists Sponsorship Program by the China Association for Science and Technology (CAST) under Grant 2018QNRC001, in part by the Applied Basic Research Project of China Textile Industry Association under Grant J201806, and in part by the Program for Innovative Research Team, University of Tianjin, under Grant TD13-5037.

ABSTRACT It is well known that the asymmetric gears of the transmission system enhances the load carrying capacity of system, but there is no relevant conclusion about the dynamic load-sharing characteristics of the asymmetric gear transmission system. In order to analyze the dynamic performance of an asymmetric gear system, taking two-stage asymmetric helical gear star drive system as the research object, the load-sharing model of the two-stage asymmetrical helical star gear system is established by the centralized mass method and Newton's second law. The load sharing characteristic of the star gear is studied about the floating member and the tooth profile pressure angle. The influence of eccentricity error, load and input speed on the load sharing performance of the system is analyzed. Based on ADAMS virtual prototype model, through the simulation analysis of the dynamic meshing force of gears, the load sharing coefficient of each star gear is calculated, compare the results with the MATLAB solution to verify the correctness of the theory.

INDEX TERMS Star gear system, asymmetrical gear, load-sharing coefficient, dynamics.

I. INTRODUCTION

In 2011, Kamel *et al.* [1] investigated the dynamic behavior of a two stage spur gear system used in a typical wind turbine. In 2012, Zhu *et al.* [2] calculated of the load sharing coefficients of the internal and external meshing, and analyzed the impact of installation errors on the load sharing characteristic. In 2013, Wei *et al.* [3] studied the effect of the meshing angle in bending-torsional coupling model on the load-sharing characteristic. In 2014, Wang *et al.* [4] analyzed the influence of revolution speed and meshing error on dynamic load sharing characteristic in multiple-stage planetary gear model. In 2015, taking eccentricity error, static transmission error and time varying meshing stiffness into consideration, Dong-ping *et al.* [5] proposed a new bending-torsional coupling model. Qiu *et al.* [6] investigated the load-sharing dynamic characteristics of a rotational-translational-axial planetary gear model; Wu *et al.* [7] set up a non-linear dynamics model of Ravigneaux compound planetary gear sets and obtained the relationships between the mesh errors and the load sharing coefficients. In 2016, Mo *et al.* [8], [9] proposed a new dynamic model for double-helical star gearing system, considering multiple errors and obtained the values and the vibration mode for different order. In 2017, taking the comprehensive angle meshing error into consideration, Shuai *et al.* [10] obtained the regular curves of the load sharing coefficient. Mo *et al.* [11] made mechanism analysis on load sharing behavior among star gears of star gearing reducer; Leque and Kahraman [12] developed the load sharing model to show combined errors influence on load sharing characteristic. Iglesias *et al.* [13] researched the effect of manufacturing errors on the quasi-static behavior considering the bearing condition of the sun gear shaft. In 2018, Zhang *et al.* [14] completed the optimal design of

The associate editor coordinating the review of this manuscript and approving it for publication was Hassan Ouakad.

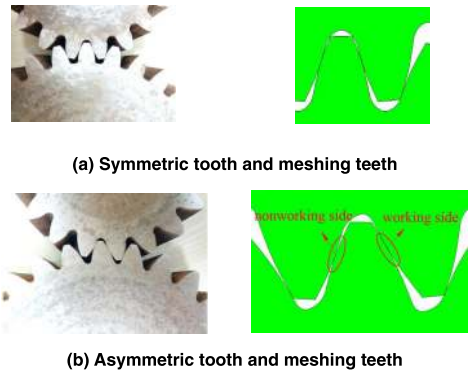

(a) Symmetric tooth and meshing teeth

(b) Asymmetric tooth and meshing teeth

FIGURE 1. Symmetric gear and asymmetric gear.

the dynamic load sharing performance for an in-wheel motor planetary gear reducer; Kim *et al.* [15] thought reducing planetary pin diameter and increasing planetary bearing clearance can approve load sharing among the planetary gears; Xu *et al.* [16] established a 21 degree of freedom lumped parameters dynamical model to study the dynamical load sharing behaviors.

The research object of dynamics and load sharing characteristics is the transmission system of the traditional gear set. The main research direction is focused on the complete error analysis and the complicated structure of the system. So we combine asymmetric gear and star gear system. The advantage is that the asymmetric gear is pulled in the trans system to establish a model for the asymmetric gear star system. The literature on the dynamics of the asymmetric gear system is as follows:

In 2008, Karpat *et al.* [17] used the method of dynamic analysis to compare conventional spur gears with symmetric teeth and spur gears with asymmetric teeth about the dynamic factor. In 2012, Ning and Wei [18] used MSC.ADAMS software to analyze the dynamic performance of asymmetric gear system; In 2015, Deng *et al.* [19] researched the mesh stiffness of unmodified and modified asymmetric spur gears; In 2017, Karpat *et al.* [20] developed a new method to calculate the meshing stiffness of asymmetric gears.

By consulting the literature, we find that the research on the load sharing characteristics of asymmetric gear transmission systems is in the blank. Therefore, the two-stage asymmetric helical gear star transmission system and load sharing characteristics are studied. The dynamic load generated by each component and the influence of error on load sharing performance are analyzed and a method is proposed to improve load sharing performance.

II. ASYMMETRIC STAR SYSTEM MODEL

As shown in figure 1, due to the different pressure angles on both sides of the tooth profile, the tooth tip of the asymmetric gear is thinner and the root becomes thicker from the appearance. In figure 1 (a) and (b), the picture in the middle is the gear sample we processed. In the asymmetric gear transmission process, the large pressure angle side is

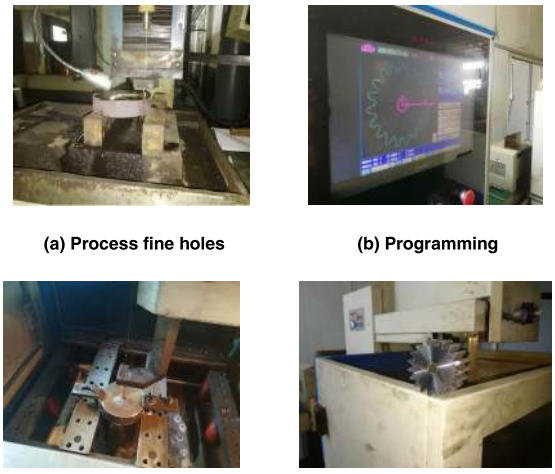

(a) Process fine holes (b) Programming

(c) Wire cutting (d) Sample

FIGURE 2. Processing of asymmetric gear.

(a) 20°/20° (b) 20°/25° (c) 20°/30°

FIGURE 3. Asymmetric gear sample.

the driving side, and the power is transmitted by the contact with the large pressure angle side of the other asymmetric gear, and the small pressure angle side is the non-driving side. Due to the change in the pressure angle of the asymmetric gear, the magnitude and direction of the component force in the x, y axis direction are changed, thereby affecting the load sharing performance of the planetary gears in the transmission system. Therefore, the asymmetric gear transmission is only suitable for the transmission system with one-way transmission power.

We completed early the design method [21] and machining of the asymmetric gear. In the processing of machining asymmetric involute gears, in order to highlight the difference in the micromorphology of the asymmetric gears, three sets of asymmetric gears with a combination of pressure angles (nonworking side/ working side) are are made into 20°/20°, 20°/25° and 20°/30°. The blanks are machined into fine holes for easy positioning, and import the drawings into the control unit, automatic programming, after the workpiece is fixed, the WEDM is processed to form a sample, The process is shown in figure 2 and the samples are shown in figure 3.

Based on the completion of the design method and machining, the bending strength of asymmetric gear pair is studied and verified. The result shows that the asymmetric gear pair can improve the bearing capacity of the gear. Next, the superiority of the asymmetric gear system from the perspective

TABLE 1. Parameters of two stage star gear transmission system.

Type	Tooth number	Modulus (mm)	Helix angle (β)	AGSPA (°)	SGSPA (°)	Torque (Nm)
Z_I	160					
Z_{p1i}	40	3	12.18	20/30	20/20	3×10^5
Z_{p2i}	80					
Z_S	40					

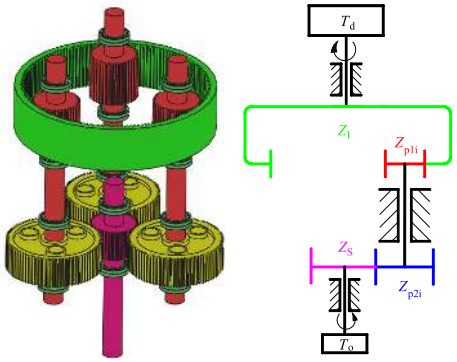

FIGURE 4. Structure and 3D model of a two stage asymmetrical star gear system.

of dynamics is researched, and the relationship about kinetic influence factors is studied.

A two-stage asymmetric star gear transmission system model is established based on previous works. The main parameters of the star gear system are shown in Table 1. AGSPA is the abbreviation of the pressure angle of the asymmetric gear system, and SGSPA is the abbreviation of the symmetrical gear system.

The physical model of the two-stage asymmetric star gear transmission system is shown in Figure 4. The input torque T_d is transmitted to the first stage three small star gears Z_{p1i} through the internal gear Z_I, and then transmitted to the sun gear Z_S through the second stage three large star gears Z_{p2i}. The sun gear outputs torque is noted as T_o. There are radial, tangential and torsional fluctuations in internal gears, large (small) star gears and sun gears, which can reduce the impact between the components and can promote the load distributed uniformly in the star gear.

III. MESHING ERROR ANALYSIS

A. EQUIVALENT MESHING ERROR

Various errors are projected onto the meshing line, and the direction away from the meshing line is taken as the positive direction of the meshing line error. Figure 5 shows manufacturing errors E and installation errors A, γ indicates the initial angle of manufacturing error, β indicates the initial angle of the installation error, o indicates the theoretical center of the system, and o' indicates the true center of the system.

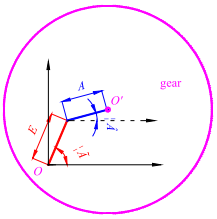

FIGURE 5. Manufacturing and installation error.

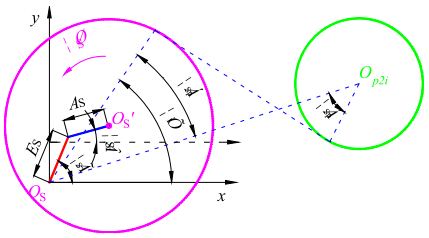

FIGURE 6. Manufacturing and installation error of sun gear.

Figure 6 shows the projection of the manufacturing error of the sun gear in the direction of the mesh line; φ_{ESi} represents the angle between the E_S and the meshing line; φ_{ASi} represents the angle between the A_S and the meshing line. ω represents the angular velocity of rotation; α_{Sp} represents the meshing angle of the external meshing drive, α_{Ip} represents the meshing angle of the internal meshing drive; φ_i represents the angle between the i-th star gear and the first large star gear, the expression of which is $\varphi_i = 2\pi\ (i\text{-}1)\ /\ N$, N represents the number of large (small) star gears, subscript S, $p1i$, $p2i$ and I refer to the sun gear, the i-th small star gear, the i-th star gear and the internal gear. The expressions of φ_{ESi} and φ_{ASi} are:

$$\begin{cases} \varphi_{ESi} = \omega_S t + \gamma_S + \alpha_{Sp} - \varphi_i \\ \varphi_{ASi} = \beta_S + \alpha_{Sp} - \varphi_i \end{cases} \tag{1}$$

The equivalent mesh errors of E_S and A_S along the meshing line are,

$$\begin{cases} e_{ESi} = -E_S \sin(\omega_S t + \gamma_S + \alpha_{Sp} - \varphi_i) \\ e_{ASi} = -A_S \sin(\beta_S + \alpha_{Sp} - \varphi_i) \end{cases} \tag{2}$$

where, e_{ESi} is the projection of the manufacturing error of the sun gear in the direction of the mesh line, e_{ASi} is the projection of the installation error of the sun gear in the direction of the mesh line, E_{bS} is the manufacturing error of the bearing supporting the sun gear; e_{EbS} is the projection of the manufacturing error of the bearing supporting the sun gear in the direction of the i-th large star gear mesh line.

$$e_{EbSi} = -E_{bS} \sin(\omega_S t + \gamma_S + \alpha_{Sp} - \varphi_i) \tag{3}$$

Figure 7 shows the projection of the manufacturing error of the internal gear in the direction of the mesh line. φ_{EIi} represents the angle between E_I and the meshing line; φ_{AIi} represents the angle between A_I and the meshing line.

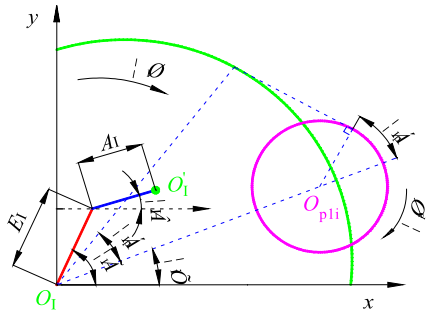

FIGURE 7. Manufacturing and installation error of internal gear.

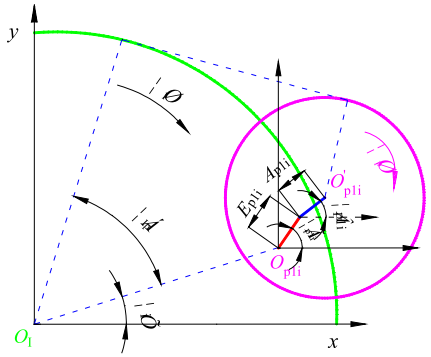

FIGURE 8. Manufacturing and installation error of i-th small star gear.

The expression of the φ_{EIi} and φ_{AIi} are:

$$\begin{cases} \varphi_{EIi} = \omega_I t + \gamma_I - \alpha_{Ip} - \varphi_i \\ \varphi_{AIi} = \beta_I - \alpha_{Ip} - \varphi_i \end{cases} \tag{4}$$

The equivalent mesh error along the meshing line of E_{I} and A_{I} are:

$$\begin{cases} e_{EIi} = -E_I \sin(\omega_I t + \gamma_I - \alpha_{Ip} - \varphi_i) \\ e_{AIi} = -A_I \sin(\beta_I - \alpha_{Ip} - \varphi_i) \end{cases} \tag{5}$$

where, e_{EIi} is the projection of the manufacturing error of the internal gear in the direction of the mesh line, e_{AIi} is the projection of the installation error of the internal gear in the direction of the mesh line. E_{bI} is the manufacturing error of bearing supporting internal gear; e_{EbI} is the projection of the manufacturing error of the bearing supporting internal gear in the direction of the i-th small star gear mesh line.

$$e_{EbIi} = -E_{bI} \sin(\omega_I t + \gamma_I - \alpha_{Ip} - \varphi_i) \tag{6}$$

Figure 8 shows the projection of the manufacturing error of i-th small star gear in the direction of the mesh line. φ_{EIpi} represents the angle between E_{p1i} and the meshing line; φ_{AIpi} represents the angle between A_{I} and the meshing line. The expression of φ_{EIpi} and φ_{AIpi} are:

$$\begin{cases} \varphi_{EIpi} = \omega_p t + \gamma_{p1i} - \alpha_{Ip} - \varphi_i \\ \varphi_{AIpi} = \beta_{p1i} - \alpha_{Ip} - \varphi_i \end{cases} \tag{7}$$

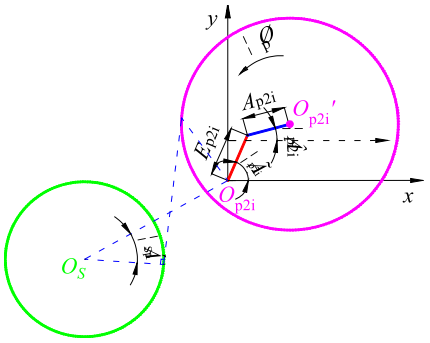

FIGURE 9. Diagram of manufacturing error and installation error of i-th large star gear.

The equivalent mesh error along the meshing line of E_{p1i} and A_{p1i} are:

$$\begin{cases} e_{Ep1i} = E_{p1i} \sin(\omega_p t + \gamma_{p1i} - \alpha_{Ip} - \varphi_i) \\ e_{Ap1i} = A_{p1i} \sin(\beta_{p1i} - \alpha_{Ip} - \varphi_i) \end{cases} \tag{8}$$

where, e_{Ep1i} is the projection of the manufacturing error of i-th small star gear in the direction of the mesh line; e_{Ap1i} the projection of the installation error of i-th small star gear in the direction of the mesh line. E_{bp1i} is the manufacturing error of bearing supporting i-th small star gear; e_{Ebp1i} is the projection of the manufacturing error of the bearing supporting i-th small star gear in the direction mesh line.

$$e_{Ebp1i} = -E_{bp1i} \sin(\omega_p t + \gamma_{p1i} + \alpha_{Ip} - \varphi_i) \tag{9}$$

Figure 9 shows the projection of the manufacturing error of i-th large star gear in the direction of the mesh line. φ_{ESpi} represents the angle between E_{p2i} and the meshing line; φ_{ASpi} represents the angle between A_{S} and the meshing line. The expression of φ_{ESpi} and φ_{ASpi} are:

$$\begin{cases} \varphi_{ESpi} = \omega_p t + \gamma_{p2i} + \alpha_{Sp} - \varphi_i \\ \varphi_{ASpi} = \beta_{p2i} + \alpha_{Sp} - \varphi_i \end{cases} \tag{10}$$

The equivalent mesh error along the meshing line of E_{p2i} and A_{p2i} are

$$\begin{cases} e_{Ep2i} = E_{p2i} \sin(\omega_p t + \gamma_{p2i} + \alpha_{Sp} - \varphi_i) \\ e_{Ap2i} = A_{p2i} \sin(\beta_{p2i} + \alpha_{Sp} - \varphi_i) \end{cases} \tag{11}$$

where, e_{Ep2i} is the projection of the manufacturing error of i-th large star gear in the direction of the mesh line; e_{Ap2i} is the projection of the installation error of i-th large star gear in the direction of the mesh line.

E_{bp2i} is the manufacturing error of bearing supporting i-th large star gear; e_{Ebp2i} is the projection of the manufacturing error of the bearing supporting i-th large star gear in the direction mesh line.

$$e_{Ebp2i} = -E_{bp2i} \sin(\omega_p t + \gamma_{p2i} + \alpha_{Sp} - \varphi_i) \tag{12}$$

where, e_{pS} is the base pitch error of sun gear, e_{pI} is the base pitch error of internal gear, e_{ppS} is the base pitch error of large star gear, e_{ppI} is the base pitch error of small star gear. ζ_{S} is

the tooth profile error of sun gear, ζ_{I} is the tooth profile error of internal gear, ζ_{p1i} is the tooth profile error of i-th large star gear, ζ_{p2i} is the tooth profile error of i-th small star gear.

B. CUMULATIVE MESHING ERROR

e_{S} is the cumulative meshing error of first stage internal-star gear transmission in asymmetric gear system; e_{I} is the cumulative meshing error of second stage sun-star gear transmission in asymmetric gear system. The cumulative meshing error of first stage internal-star gear:

$$e_{Ii} = (e_{EIi} + e_{EbIi} + e_{Ep1i} + e_{Ebp1i} + e_{AIi} + e_{Ap1i} + e_{pI} + e_{pp1i} + \xi_I + \xi_{p1i}) \cos\beta_b \quad (13)$$

The cumulative meshing error of second stage sun-star gear:

$$e_{Si} = (e_{ESi} + e_{EbSi} + e_{Ep2i} + e_{Ebp2i} + e_{ASi} + e_{Ap2i} + e_{pS} + e_{pp2i} + \xi_S + \xi_{p2i}) \cos\beta_b \quad (14)$$

IV. LOAD SHARING MODEL

Establish the coordinate system: $Oxyz$ is the fixed coordinate system, the origin is the rotation center of the internal gear and the sun gear, the internal gear rotates with an the angular velocity w_{I}, the sun gear rotates with an the angular velocity w_{S}; $O_{\mathrm{p1i}}x_{\mathrm{p1i}}y_{\mathrm{p1i}}z_{\mathrm{p1i}}$ is the fixed coordinate system, the origin is the rotation center of the small star gear, $i = 1, 2, 3$; $O_{\mathrm{p2i}}x_{\mathrm{p2i}}y_{\mathrm{p2i}}z_{\mathrm{p2i}}$ is the fixed coordinate system, the origin is the center of rotation of the large star gear. Micro-displacements along the x, y and z axes and the angular displacement around the z-axis of each gear are considered, respectively.

The internal gear is a thin-walled cylindrical structure with three translations of x, y and z axes and angular displacements around the z-axis, a total of four degrees of freedom; the large (small) star and the sun gear also have four degrees of freedom. The system has a total of $(8 + 8N)$ degrees of freedom, N is the number of large (small) stars and X is the displacement matrix for asymmetric star gear system:

$$X = [u_{\mathrm{I}}, x_{\mathrm{I}}, y_{\mathrm{I}}, z_{\mathrm{I}}, u_{\mathrm{S}}, x_{\mathrm{S}}, y_{\mathrm{S}}, z_{\mathrm{S}}, u_{\mathrm{p1i}}, x_{\mathrm{p1i}}, y_{\mathrm{p1i}}, z_{\mathrm{p1i}}, u_{\mathrm{p2i}}, x_{\mathrm{p2i}}, y_{\mathrm{p2i}}, z_{\mathrm{p2i}}]$$

where,x, y and z represent the micro-displacement of the component, u indicates the torsional displacement of the component. $u_{\mathrm{I}} = \theta r_{\mathrm{b}}$, in this equation, r_{b} represents the base circle radius and θ represents the rotational angle of each gear. Figure 10 shows the 3D dynamic model of asymmetric star gear system, which is established based on the centralized mass method. In this model, each component is regarded as a rigid body. The sun gear, internal gear and star gear in system are all set as floating components. Also, the influence of the meshing stiffness, support stiffness, meshing damping and meshing errors are taken into consideration in this model. Figure 11 and Figure 12 show these dynamic models.

K_{Sp}, K_{IP} represent the average meshing stiffness between the sun gear and the large star gear, the internal gear and the small star gear respectively; C_{Sp}, C_{IP} represent the meshing damping between the sun gear and the large star gear, the internal gear and the small star gear respectively; K_{S}, K_{I}, K_{p} respectively represent the support stiffness of the sun gear, the internal gear, small star gear and large star gear; $K_{1\mathrm{t}}$, $K_{2\mathrm{t}}$, $K_{3\mathrm{t}}$ represent the coupled torsional stiffness of the i-th double star gear.

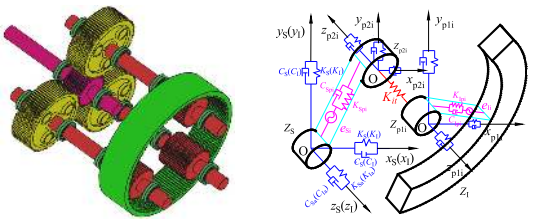

FIGURE 10. Dynamic model of asymmetric star gear system.

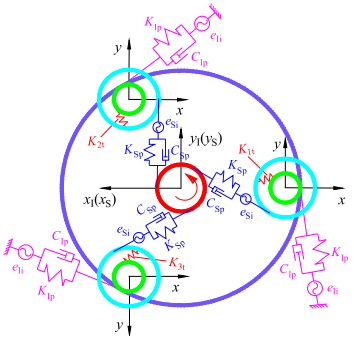

FIGURE 11. Load sharing dynamic model of two stage asymmetrical star gear system.

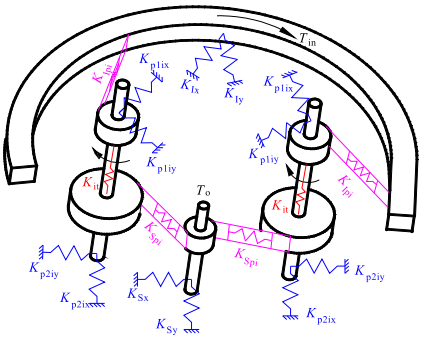

FIGURE 12. Mechanical model of two-stage asymmetric gear transmission system.

$$\begin{cases} \mu_{Spi} = (-r_{p2i}u_{p2i} - r_S u_S + (x_{p2i} - x_S)\sin A_i \\ +(y_{p2i} - y_S)\cos A_i)\sin\beta \\ +(-z_S + z_{p2i})\cos\beta + e_{Si} \\ \mu_{Ipi} = (r_I u_I - r_{p1i}u_{p1i} + (x_I - x_{p1i})\sin B_i \\ +(y_{p1i} - y_I)\cos B_i)\sin\beta \\ +(z_I - z_{p1i})\cos\beta + e_{Ii} \end{cases} \quad (15)$$

where, μ_{Spi} represents the equivalent displacement difference of the i-th large star gear and the sun gear on the meshing line, and μ_{Ipi} represents the equivalent displacement of the

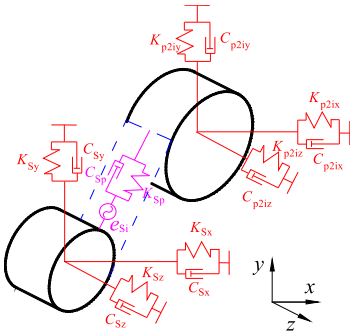

FIGURE 13. Dynamic model of sun-star gear pair.

i-th small star gear and the internal gear on the meshing line.

$$\begin{cases} F_{Spi} = K_{Spi}\mu_{Spi} \\ F_{Ipi} = K_{Ipi}\mu_{Ipi} \\ D_{Spi} = C_{Spi}\dot{\mu}_{Spi} \\ D_{Ipi} = C_{Ipi}\dot{\mu}_{Ipi} \end{cases} \tag{16}$$

where, F_{Spi} is the meshing force of sun-star pair with i-th star gear, F_{Ipi} is the meshing force of internal-star pair with i-th star gear, D_{Spi} is the meshing damping of sun-star pair with i-th star gear, D_{Ipi} is the meshing damping of sun-star pair with i-th star gear.

A. FORCE BALANCE EQUATION OF THE SUN GEAR

Figure 13 shows the dynamic model of a sun-star pair with i-th star gear in star gear system. The force balance equation of the sun gear is:

$$\begin{cases} m_S\ddot{x}_S - \sum_{i=1}^{3}(F_{Sp2i} + D_{Sp2i})\sin A_i\cos\beta \\ +K_{Sx}x_S + C_{Sx}\dot{x}_S = 0 \\ m_S\ddot{y}_S - \sum_{i=1}^{3}(F_{Sp2i} + D_{Sp2i})\cos A_i\cos\beta \\ +K_{Sy}y_S + C_{Sy}\dot{y}_S = 0 \\ m_S\ddot{z}_S - \sum_{i=1}^{3}(F_{Sp2i} + D_{Sp2i})\sin\beta \\ +K_{Sz}z_S + C_{Sz}\dot{z}_S = 0 \\ J_S\ddot{u}_S - \sum_{i=1}^{3}(F_{Sp2i} + D_{Sp2i})r_S\cos\beta \\ +K_{St}u_S = -T_o \end{cases} \tag{17}$$

B. FORCE BALANCE EQUATION OF THE LARGE STAR GEAR

Figure 14 shows the dynamic model of a double star gear in star gear system. K_{it} are the coupling stiffness for i-th star gear. The equilibrium equations of the second stage large star

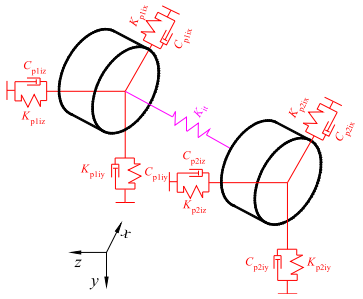

FIGURE 14. Dynamic model of double star gear.

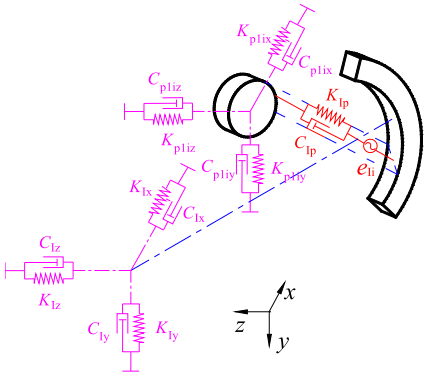

FIGURE 15. Dynamic model of internal-star gear pair.

gear are:

$$\begin{cases} m_{p2i}\ddot{x}_{p2i} + (F_{Sp2i} + D_{Sp2i})\sin A_i\cos\beta \\ +K_{p2ix}x_{p2i} + C_{p2ix}\dot{x}_{p2i} = 0 \\ m_{p2i}\ddot{y}_{p2i} + (F_{Sp2i} + D_{Sp2i})\cos A_i\cos\beta \\ +K_{p2iy}y_{p2i} + C_{p2iy}\dot{y}_{p2i} = 0 \\ m_{p2i}\ddot{z}_{p2i} + (F_{Sp2i} + D_{Sp2i})\sin\beta \\ +K_{p2iz}z_{p2i} + C_{p2iz}\dot{z}_{p2i} = 0 \\ J_{p2i}\ddot{u}_{p2i} + (F_{Sp2i} + D_{Sp2i})r_{p2i}\cos\beta \\ +K_{p2it}u_{p2i} + K_{it}(u_{p2i} - u_{p1i}) = 0 \end{cases} \tag{18}$$

C. FORCE BALANCE EQUATION OF THE SMALL STAR GEAR

The equilibrium equations of the first stage small star gear are

$$\begin{cases} m_{p1i}\ddot{x}_{p1i} - (F_{Sp1i} + D_{Sp1i})\sin A_i\cos\beta \\ +K_{p1ix}x_{p1i} + C_{p1ix}\dot{x}_{p1i} = 0 \\ m_{p1i}\ddot{y}_{p1i} + (F_{Sp1i} + D_{Sp1i})\cos A_i\cos\beta \\ +K_{p1iy}y_{p1i} + C_{p1iy}\dot{y}_{p1i} = 0 \\ m_{p1i}\ddot{z}_{p1i} - (F_{Sp1i} + D_{Sp1i})\sin\beta \\ +K_{p1iz}z_{p1i} + C_{p1iz}\dot{z}_{p1i} = 0 \\ J_{p1i}\ddot{u}_{p1i} - (F_{Sp1i} + D_{Sp1i})r_{p1i}\cos\beta \\ +K_{p1it}u_{p1i} + K_{it}(u_{p1i} - u_{p2i}) = 0 \end{cases} \tag{19}$$

D. FORCE BALANCE EQUATION OF THE INTERNAL GEAR

Figure 15 shows the dynamic model of an internal-star pair with i-th star gear in star gear system. The equilibrium

equations of internal gear are:

$$\begin{cases} m_I \ddot{x}_I + \sum_{i=1}^{3} (F_{Ip1i} + D_{Ip1i}) \sin A_i \cos \beta \\ +K_{Ix} x_I + C_{Ix} \dot{x}_I = 0 \\ m_I \ddot{y}_I - \sum_{i=1}^{3} (F_{Ip1i} + D_{Ip1i}) \cos A_i \cos \beta \\ +K_{Iy} y_I + C_{Iy} \dot{y}_I = 0 \\ m_I \ddot{z}_I - \sum_{i=1}^{3} (F_{Ip1i} + D_{Ip1i}) \sin \beta \\ +K_{Iz} z_I + C_{Iz} \dot{z}_I = 0 \\ J_I \ddot{u}_I + \sum_{i=1}^{3} (F_{Ip1i} + D_{Ip1i}) r_I \cos \beta \\ +K_{It} u_I = T_{in} \end{cases} \tag{20}$$

In Equation (17) - Equation (20), m represents the mass of gear, J represents moment of inertia of the gear, T_o represents the output torque, T_{in} represents the input torque. x represents the displacement in the x-direction of the gear, y represents the displacement in the y-direction of the gear, z represents the displacement in the z-direction of the gear, and u represents the torsional displacement in the z-direction of the gear.

V. LOAD SHARING COEFFICIENT CALCULATION

This paper takes the planetary transmission system in a wind turbine as the research object. Table 2 shows the initial values of these gears' parameter and the manufacturing errors of the sun gear, the internal gear and the star gear. In addition, all the other errors are 6 μm.

The load sharing coefficient represents the distribution of load on each star gear in transmission system. The definition equations are shown in equations (21) and (22). Similarly, the maximum value of each star gear's load sharing coefficient is defined as the load sharing coefficient of the star gear transmission system. The definition equations are shown in equations (23) and (24).

$$\Omega_{Ipi} = \frac{NF_{Ipi}}{\sum_{i=1}^{N} F_{Ipi}} \tag{21}$$

$$\Omega_{Spi} = \frac{NF_{Spi}}{\sum_{i=1}^{N} F_{Spi}} \tag{22}$$

$$\Omega_{Ip} = (\Omega_{Ipi})_{\max} = \frac{N(F_{Ipi})_{\max}}{\sum_{i=1}^{N} F_{Ipi}} \tag{23}$$

$$\Omega_{Sp} = (\Omega_{Spi})_{\max} = \frac{N(F_{Spi})_{\max}}{\sum_{i=1}^{N} F_{Spi}} \tag{24}$$

Taking the star gear system model as an example, the internal and external meshing forces of each star gear in equations (15) – (20) can be solved by ODE45 in MATLAB, and then the load sharing coefficient of the first and second stage system can be solved according to equations (21) – (24). The curves of load sharing coefficient are shown in Figure 16 and Figure 17; while the meshing force of gear pairs are shown in Figure 18 and Figure 19.

TABLE 2. Calculated stiffness values.

Parameters	Unit	Z_I	Z_{p1i}	Z_{p2i}	Z_S
Teeth	/	160	40	80	40
Normal modulus	mm	3	3	3	3
Pressure angle	°	20/30	20/30	20/30	20/30
Helical angle	°	12.18	12.18	12.18	12.18
Meshing stiffness	N/m	2×10^10		1×10^10	
Supporting stiffness	N/m	1×10^13	1×10^13	2×10^13	2×10^13
Meshing damping	N/m·kg	1×10^6		1×10^6	
Torsional stiffness	N/m	1×10^10	1×10^10	1×10^10	1×10^10
Couple stiffness	N/m	/	1×10^10		/
Input speed	r/min	17	/	/	/
Input torque	Nm	3×10^5	/	/	/
Manufacturing error	μm	6	6	6	6
Phase	rad	0.5	0.5	0.5	0.5
Installation error	μm	6	6	6	6
Phase	rad	0.5	0.5	0.5	0.5

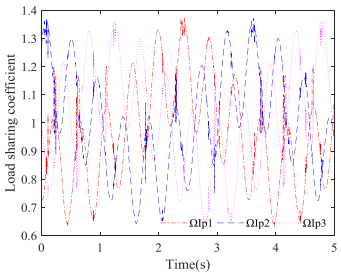

FIGURE 16. The load sharing coefficient of internal gearing transmission.

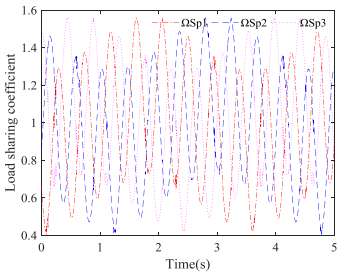

FIGURE 17. The load sharing coefficient of external gearing transmission.

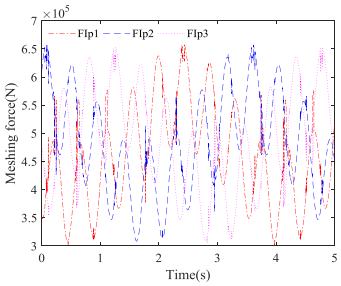

FIGURE 18. Meshing force of internal gearing transmission.

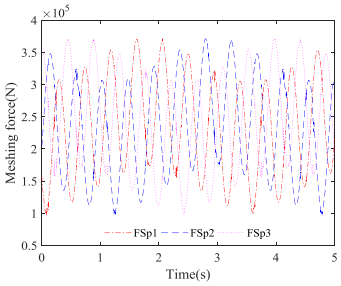

FIGURE 19. Meshing force of external gearing transmission.

TABLE 3. Load sharing coefficient when the pressure angle of the internal gear varies.

Pressure angle (°)	Load sharing coefficient	Pressure angle (°)	Load sharing coefficient
20	1.3685	28	1.3701
22	1.3792	30	1.3671
24	1.3657	32	1.3676
26	1.3710	34	1.3658

VI. LOAD SHARING COEFFICIENT ANALYSIS

A. EFFECT OF PRESSURE ANGLE ON LOAD SHARING COEFFICIENT

In Figure 16 and Figure 17, the asymmetric gear transmission system is used as a research project to obtain the load sharing coefficient of each star gear. As shown in the result, the load sharing coefficient of the first-stage internal meshing is 1.3685, and the load sharing coefficient of the second-stage external meshing is 1.5565.

With the same design, the variable is the pressure angle, and the pressure angle at the working side of the tooth profile increases from 20° to 34°. The dynamic load sharing coefficient of each star gear obtained by calculation is shown in Table 3 and Table 4.

1) The non-working side pressure angle of the internal meshing gear is maintained 20°, and the working side pressure angle is varied between 20° and 34°. The variation law of the load sharing coefficient is shown in Table 3.

2) The non-working side pressure angle of the external meshing gear is maintained 20°, and the working side pressure angle is varied between 20° and 34°. The change of the load sharing coefficient is shown in Table 4.

TABLE 4. Load sharing coefficient when the pressure angle of the sun gear varies.

Pressure angle (°)	Load sharing coefficient	Pressure angle (°)	Load sharing coefficient
20	1.5565	28	1.5563
22	1.5564	30	1.5562
24	1.5752	32	1.5562
26	1.5563	34	1.5754

As the working side pressure angle changes, the relevant parameters in the dynamic differential equation will change with it, which will affect the meshing force between the gear pairs, where the load sharing coefficient change as well. When pressure angle changes, the load sharing coefficient of the first-stage internal gear system varies between 1.36 and 1.38, and the load sharing coefficient of the second-stage external gear system changes between 1.55 and 1.58. When the pressure angle of working side changes, the load sharing coefficient of the whole system will fluctuate. But the fluctuation is small, and there is no certain rule to follow. Therefore, the change of pressure angle will lead the magnitude and direction of the load change, while has rarely effect on load sharing coefficient.

B. EFFECT OF ERROR ON LOAD SHARING COEFFICIENT

Supposed other parameters are constant values, and the pressure angle at working side is set as 30° to study the effect on load sharing coefficient by changing a certain parameter separately. In order to study the influence of error of each gear on load sharing coefficient, the load sharing coefficients are obtained by changing the errors of sun gear, internal gear, the large star gear and the small star gear respectively. These load sharing coefficients are shown in Figure 20 and Figure 21.

The change of gear manufacturing error and installation error can result the change of load sharing coefficient in the system. The error variation of the external meshing pair has a great influence on the load sharing coefficient. The load sharing coefficient increases by about 0.1 in the same error variation range, and the error of the internal meshing pair is less affected. The effect of manufacturing error on the system's load sharing coefficient is more significant than the installation error. As the manufacturing error and installation error increase, the load sharing coefficient of the system also increases. Therefore, it is necessary to control the error of the system and to reduce the fluctuation of the load sharing coefficient. Particularly, the higher the transmission level is, the more obvious the impact of the error on the load sharing coefficient impacts in the load sharing characteristics of the multi-stage transmission system.

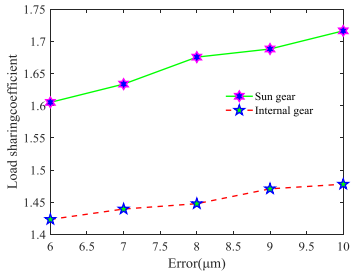

(a) Manufacturing error of center gear

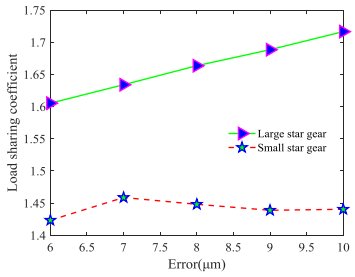

(b) Manufacturing error of star gear

FIGURE 20. Influence of manufacturing error on load sharing coefficient.

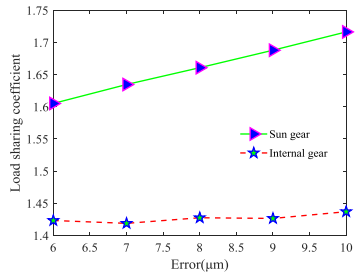

(a) Installation error of center gear

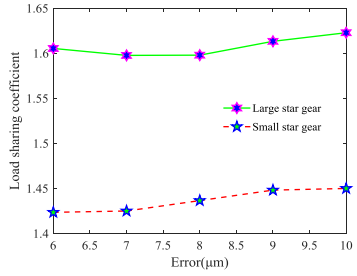

(b) Installation error of star gear

FIGURE 21. Influence of installation error on load sharing coefficient.

C. EFFECT OF STIFFNESS/DAMPING ON LOAD SHARING COEFFICIENT

The support stiffness and the meshing damping of the gear are respectively changed, and the load sharing coefficient of the system is calculated. When studying the influence of the support stiffness of the internal gear on the load sharing coefficient, the support stiffness of other gears is kept constant, and the support stiffness of the internal gear ranges from 2×10^{10} to 10×10^{10}. When studying the influence of the

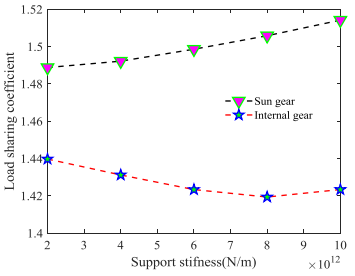

(a) Support stiffness of center gear

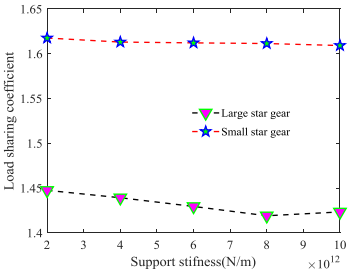

(b) Support stiffness of star gear

FIGURE 22. Influence of support stiffness on load sharing coefficient.

support stiffness of the sun gear on the load sharing coefficient, keep the support stiffness of other gears unchanged. The support stiffness of the sun gear ranges from 2×10^{10} to 10×10^{10}. The variation of the load sharing coefficient of the first-stage transmission and the second-stage transmission is shown in Figure 22.

The greater the support stiffness of the sun gear is, the greater the load sharing coefficient of the system become. And the load sharing coefficient of the second-stage transmission system is greatly affected by the support stiffness of the sun gear. The change of the support stiffness of the large star gear makes the change of the load sharing coefficient is maximum, which is decreasing by 0.025. Likewise, the sun gear increases the load sharing coefficient by 0.02, while the star gear and internal gear are just opposite. That is, with the increase of the support stiffness of the star gear and internal gear, the load sharing coefficient of the star gear is decreasing, where the range of variation is almost 0.01. AS shown in the result, the influence of the support stiffness variation of the second-stage transmission on the load sharing coefficient is more obvious.

When studying the influence of the meshing damping of the first stage drive system on the load sharing coefficient, the other parameters are kept constant, and the meshing damping of the first stage drive system ranges from 0.5×10^6 to 2.5×10^6. When studying the influence of the meshing damping of the second stage drive system on the load sharing coefficient, the other parameters are kept constant, and the meshing damping of the second stage drive system ranges from 0.5×10^6 to 2.5×10^6. The variation of the load sharing coefficient of the first-stage transmission and the second-stage transmission is shown in Figure 23.

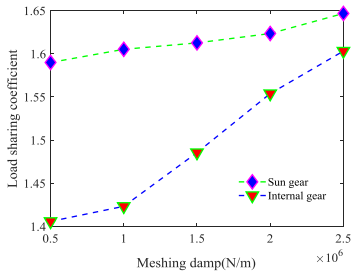

FIGURE 23. Influence of meshing damp on load sharing coefficient.

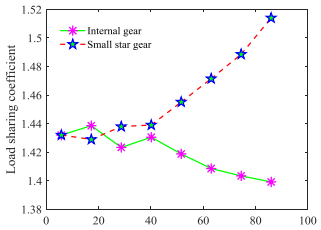

(a) Initial phase of first stage drive system

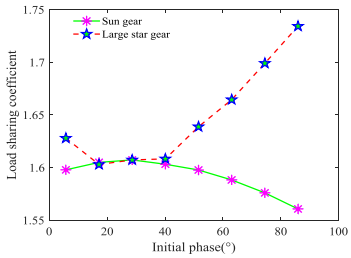

(b) Initial phase of second stage drive system

FIGURE 24. Influence of initial phase on load sharing coefficient.

In the same range of meshing damping variation, the load sharing coefficient of the first-stage transmission system is increased by 0.2, the larger the meshing damping, the faster the speed increase, and the load sharing coefficient of the second-stage transmission system is only increased by 0.06; Therefore, the change of the meshing damping has little effect on the load sharing coefficient of the second-stage transmission. The load sharing coefficient of the first-stage transmission system is more sensitive to the change of the meshing damping. In the application process, the meshing damping between the internal gear and the small star gear is reasonably selected to make the load more uniform.

D. EFFECT OF INITIAL PHASE ON LOAD SHARING COEFFICIENT

When studying the influence of initial phase of installation error on load sharing coefficient, the initial phase of other gears is kept constant, and the initial phase of the gear in first stage trans is from 0 to $\pi/2$ and the initial phase of the gear in second stage transmission is from 0 to $\pi/2$. The variation of the load sharing coefficient of the first-stage transmission and the second-stage transmission is shown in Figure 24.

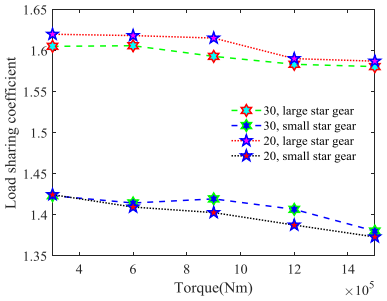

FIGURE 25. Influence of input torque on load sharing coefficient.

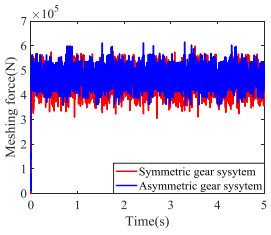

(a) First star gear

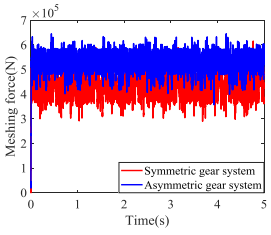

(b) Second star gear

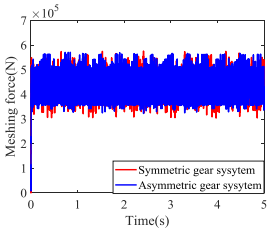

(c) Third star gear

FIGURE 26. First stage meshing force.

During the increase of initial phase of the center gear installation error, the load sharing coefficient of the first and second trans systems increases, and when the initial phase is about 30°, load sharing coefficient reaches the maximum and then gradually decreases. When the initial phase of the installation error of the star gear gradually increases, the load sharing coefficient of the system increases. So in the design of the asymmetric gear system, the initial phase angle of installation error should be reasonably selected, so that the star gear is more evenly loaded.

E. INFLUENCE OF INPUT POWER ON LOAD SHARING COEFFICIENT

In order to study the effect of input torque on the load sharing performance of the star gear transmission system,

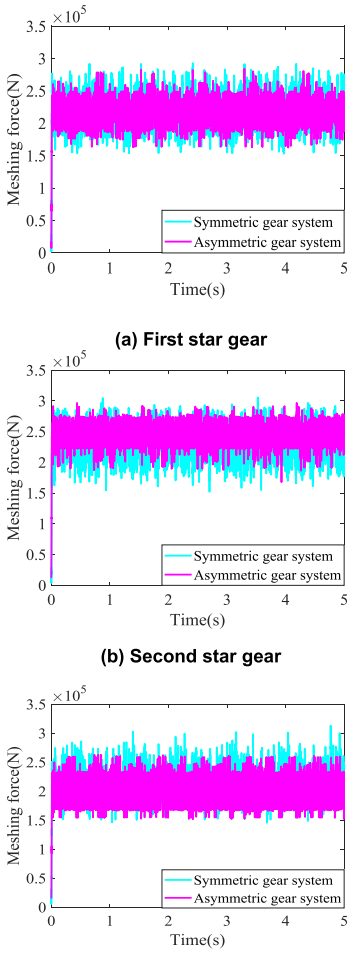

(a) First star gear

(b) Second star gear

(c) Third star gear

FIGURE 27. Second stage meshing force.

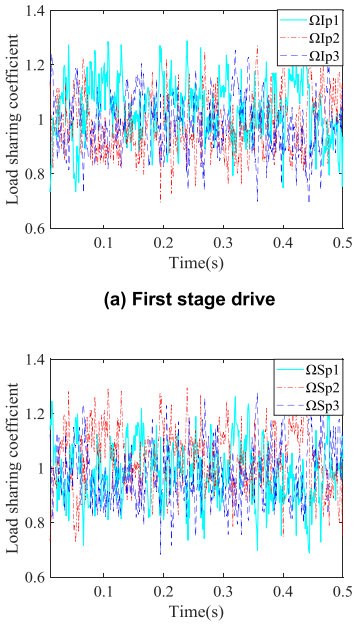

(a) First stage drive

(b) Second stage drive

FIGURE 28. Load sharing coefficient of symmetric gear system.

the parameters in Table 2 are still used. Change the input torque and calculate the load sharing coefficient of the system, as shown in Figure 25. It can be seen from Figure 25 that as the input torque increases, the load sharing coefficient of the asymmetric gear system and the symmetric gear system decreases, and their load unevenness is weakened, which is consistent with the existing research results; At the same time, the load sharing coefficient of the asymmetric gear star transmission system is smaller than that of the symmetrical gear transmission system under the same input power.

VII. DYNAMIC SIMULATION VERIFICATION

The dynamics simulation was carried out with the input speed of the wind field being 17 r/min and the rated load torque being 3.5×10^4 Nm. The stiffness coefficients of the internal and external meshing pairs are 2.85×10^{10} N/m, 3.10×10^{10} N/m, the damping is 1×10^6, the force index is 1.5, and the maximum penetration depth is 1×10^{-4} m. In order to ensure that there is no sudden change when the speed and torque are applied, the step function step () is used to increase the speed from 0 to 17 r/min in 0.01 s, and the torque increases from 0 to 3.5×10^4 Nm in 0.01 s. Set the simulation termination time to 0.5s and the simulation step size to 0.001s.

After the dynamics simulation, extract the two stage gear meshing force data in the dynamic simulation results of the wind power gear transmission system, according to the formula (21)–(24), Calculate the load sharing coefficient of the internal and external meshing gear pairs of the two stage gear transmission by MATLAB software, and obtain the meshing force of the contact pairs of the planetary gears and the center gear of the first and second transmission systems, as shown in Figure 23 and Figure 24. For the simulation results, the meshing force of the three small star gears in the first stage meshing drive is extracted as shown in Figure 26, and the meshing force of the second stage meshing is shown in Figure 27.

Figure 26 and Figure 27 show the meshing force between the planetary gear and the center gear of the symmetrical gear system and the asymmetric gear system, which is consistent with the meshing force Figure 16 and Figure 17 solved by MATLAB; Under the same working condition, the meshing force of the asymmetric gear transmission system starts from 0, and changes to value under normal working conditions within 0.01s. The variation interval of the meshing force of the asymmetric gear transmission system is smaller than the symmetrical gear transmission system, which reduces system vibration and system noise; Figure 28 and Figure 29 show the dynamic load sharing coefficient variation of the symmetrical gear system and the asymmetric gear system under dynamic simulation. Since the variation of the load sharing coefficient is periodic, it can be found in 0.5 seconds that the variation of the load sharing coefficient of the asymmetric system is smaller than that of the symmetric

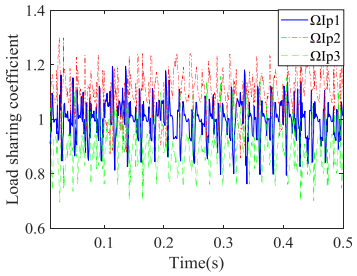

(a) First stage drive

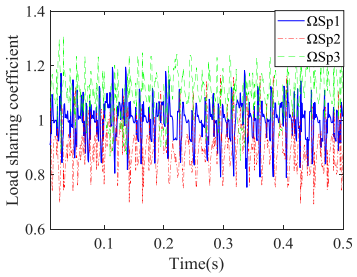

(b) Second stage drive

FIGURE 29. Load sharing coefficient of asymmetric gear system.

gear in terms of the fluctuation amplitude. The load sharing coefficient curve of the asymmetric gear system is more uniform and more regular. For any one of the planetary gears, the smaller the load sharing coefficient variation, the better the stability, and the stability of the system is enhanced.

VIII. CONCLUSION

According to the dynamic load sharing analysis model of the two-stage power split star gear transmission system, the dynamic load sharing coefficient of the two-stage asymmetric gear system is obtained, and the influences of errors, support stiffness, meshing damping coefficient and input power on the load sharing characteristics are analyzed. The conclusions are:

(1) Considering the comprehensive error of all gears, the manufacturing error of all the bearings, the two-stage asymmetric star gear system dynamic model is established according to the lumped mass method. According to the D'Alembert principle and the ODE45 module (MATLAB), the dynamic load sharing coefficient of the system is obtained.

(2) We find that the change of the pressure angle can cause the fluctuation of the load sharing coefficient of the system; the error should be controlled to minimize the error; the influence of stiffness and damping coefficient on the load sharing coefficient have different rules because of the center gear, star gear and transmission grade; The initial phase of the installation error should be considered when designing the system, and the influence of input power should also be considered.

(3) Under ADAMS simulation condition, we found that the working condition of the asymmetric gear transmission system is more stable, which is consistent with the MATLAB solution results, and demonstrates the superiority of the asymmetric gear transmission system.

REFERENCES

[1] K. Abboudi, L. Walha, M. Maatar, T. Fakhfakh, M. Haddar, and Y. Driss, "Dynamic behavior of a two-stage gear train used in a fixed-speed wind turbine," *Mech. Mach. Theory*, vol. 12, no. 46, pp. 1888–1900, Dec. 2011.

[2] Z. Zhu, R. Zhu, Y. Li, Y. Chen, and Z. Zhu, "Impact of installation error on dynamics load sharing characteristic for encased differential herringbone train," *Chin. J. Mech. Eng.*, vol. 48, no. 3, pp. 16–24, Feb. 2012.

[3] J. Wei, Q. Sun, W. Sun, X. Ding, W. Tu, and Q. Wang, "Load-sharing characteristic of multiple pinions driving in tunneling boring machine," *Chin. J. Mech. Eng.*, vol. 26, no. 3, pp. 532–540, May 2013.

[4] J. Wang, Y. Wang, and Z. Huo, "Analysis of dynamic behavior of multiple-stage planetary gear train used in wind driven generator," *Sci. World J.*, vol. 2014, Jan. 2014, Art. no. 627045.

[5] D.-P. Sheng, R.-P. Zhu, F.-X. Lu, H.-Y. Bao, and G.-H. Jin, "Dynamic load sharing characteristics and sun gear radial orbits of double-row planetary gear train," *J. Central South Univ.*, vol. 22, no. 10, pp. 3806–3816, Oct. 2015.

[6] X. Qiu, Q. Han, and F. Chu, "Load-sharing characteristics of planetary gear transmission in horizontal axis wind turbines," *Mech. Mach. Theory*, vol. 92, pp. 391–406, Oct. 2015.

[7] S. Wu, Z. Peng, and X. Wang, "Impact of mesh errors on dynamic load sharing characteristics of compound planetary gear sets," *J. Mech. Eng.*, vol. 51, no. 3, pp. 29–36, Feb. 2015.

[8] M. Shuai, Z. Yidu, and W. Qiong, "Research on natural characteristics of double-helical star gearing system for GTF aero-engine," *Mech. Mach. Theory.*, vol. 106, pp. 166–189, Dec. 2016.

[9] S. Mo, Y. Zhang, Q. Wu, S. Matsumura, and H. Houjoh, "Load sharing behavior analysis method of wind turbine gearbox in consideration of multiple-errors," *Renew. Energy*, vol. 97, pp. 481–491, Nov. 2016.

[10] S. Mo, S. Ma, G. Jin, Y. Zhang, C. Lv, and H. Houjoh, "Research on multiple-split load sharing characteristics of 2-stage external meshing star gear system in consideration of displacement compatibility," *Math. Problems Eng.*, vol. 2017, Dec. 2017, Art. no. 1037479.

[11] S. Mo, Y. Zhang, Q. Wu, F. Wang, S. Matsumura, and H. Houjoh, "Load sharing behavior of star gearing reducer for geared turbofan engine," *Chin. J. Mech. Eng.*, vol. 30, no. 4, pp. 796–803, Jul. 2017.

[12] N. Leque and A. Kahraman, "A three-dimensional load sharing model of planetary gear sets having manufacturing errors," *J. Mech. Des.*, vol. 139, no. 3, 2017, Art. no. 033302.

[13] M. Iglesias, A. F. del Rincon, A. de-Juan, P. Garcia, A. Diez-Ibarbia, and F. Viadero, "Planetary transmission load sharing: Manufacturing errors and system configuration study," *Mech. Mach. Theory*, vol. 111, pp. 21–38, May 2017.

[14] J. Zhang, X. Qin, C. Xie, and L. Jin, "Optimization design on dynamic load sharing performance for an in-wheel motor speed reducer based on genetic algorithm," *Mech. Mach. Theory*, vol. 122, pp. 132–147, Apr. 2018.

[15] J.-G. Kim, Y.-J. Park, S.-D. Lee, J.-Y. Oh, J.-H. Kim, and G.-H. Lee, "Influence of the carrier pinhole position errors on the load sharing of a planetary gear train," *Int. J. Precis. Eng. Manuf.*, vol. 19, no. 4, pp. 537–543, Apr. 2018.

[16] X. Xu, T. Luo, J. Luo, X. Hua, and R. Langari, "Dynamical load sharing behaviors of heavy load planetary gear system with multi-floating components," *Int. J. Model. Simul. Sci. Comput.*, vol. 9, no. 1, pp. 1–13, Feb. 2018.

[17] F. Karpat, S. Ekwaro-Osire, K. Cavdar, and F. C. Babalik, "Dynamic analysis of involute spur gears with asymmetric teeth," *Int. J. Mech. Sci.*, vol. 50, no. 12, pp. 1598–1610, Dec. 2008.

[18] N. Li and W. Li, "Research on meshing theory of involute helical gear with asymmetric," in *Proc. ICMST*, Singapore, 2011, pp. 2838–2844.

[19] X.-H. Deng, L. Hua, and X.-H. Han, "Characteristic of involute slope modification of asymmetric spur gear," *J. Central South Univ.*, vol. 22, no. 5, pp. 1676–1684, May 2015.

[20] F. Karpat, O. Dogan, C. Yuce, and S. Ekwaro-Osire, "An improved numerical method for the mesh stiffness calculation of spur gears with asymmetric teeth on dynamic load analysis," *Adv. Mech. Eng.*, vol. 9, no. 8, pp. 1–12, Aug. 2017.

[21] M. Shuai, M. Shuai, J. Guoguang, G. Jiabei, Z. Ting, and Z. Shengping, "Design principle and modeling method of asymmetric involute internal helical gears," *Proc. Inst. Mech. Eng. C, J. Mech. Eng. Sci.*, vol. 233, no. 1, pp. 244–255, Jan. 2019.

MO SHUAI was born in 1987. He received the Ph.D. degree in mechanical design and theory from Beihang University, Beijing, China. He is currently a Master Tutor with the Tianjin Key Laboratory of Advanced Mechatronics Equipment Technology, Tianjin Polytechnic University. His research interests include the dynamics of gear systems, planetary gear transmission, and gearbox.

MA SHUAI was born in 1993. He received the M.S. degree in mechanical design and theory from the Tianjin Key Laboratory of Advanced Mechatronics Equipment Technology, Tianjin Polytechnic University. His research interests include the precision gear transmission, transmission system design method, and load sharing characteristics.

JIN GUO GUANG was born in 1963. He received the Ph.D. degree in mechanical design and theory from Tianjin University, Tianjin, China. He is currently a Professor with the Tianjin Key Laboratory of Advanced Mechatronics Equipment Technology, Tianjin Polytechnic University. His research interests include the dynamics of gear systems, modern institutional science, and mechanical multibody system dynamics and control.

YUE ZONG XIANG was born in 1995. He is currently pursuing the M.S. degree in mechanical design and theory with Tianjin Polytechnic University. His research interests include face gear profile design, face gear dynamics, and load sharing characteristics.